Int. J.Nano Dimens. 6(1): 39-44, Winter 2015
ISSN: 2008-8868

Contents list available at **IJND**

International Journal of Nano Dimension

Journal homepage: *www.IJND.ir*

Fabrication and nano structural study on La_2O_3-Co_3O_4-ZrO_2 composite

N. Aghaeenejad[1]
A. Bahari[2]
M. Riazian[3,*]
M. Ghanbari[4]

[1]Department of Physics, Mazandaran Science and Research Branch, Islamic Azad University, Mazandaran, Iran.
[2]Department of Physics, University of Mazandaran, Babolsar, Iran.
[3]Department of Engineering, Tonekabon branch, Islamic Azad University, Tonekabon, Iran.
[4]Department of Physic, Islamic Azad University, Centeral Tehran Branch, Iran.

Received 17 August 2013
Accepted 02 December 2013

* Corresponding author:
M. Riazian
Department of Engineering, Tonekabon branch, Islamic Azad University, Tonekabon, Iran.
Tel +98 9120116905
Fax +98 1924274415
Email m.riazian@toniau.ac.ir

ABSTRACT

We report on the synthesis, morphology, chemically and structurally of La_2O_3-Co_3O_4-ZrO_2 nanostructure. The La_2O_3-Co_3O_4-ZrO_2 nanostructure was synthesized by a method based on the co-precipitation. Composite powders have been characterized by XRD (X-ray diffraction), SEM (scanning electron microscopy) and BET (Brunauer-Emmett-Teller). X-ray diffraction showed the formation of nano crystalline, $La_2Zr_2O_7$, ZrO_2, $La(OH)_3$ and Co_3O_4 phases. Scanning electron microscopy revealed that nanostructure formed by increasing the calcinations temperatures. With BET and BJH (Barrett, Joyner and Halenda) method the pore size distribution was determined. The effects of chemical compositions and calcinations temperature on the surface topography and the crystallization of phases were studied. The lattice strain of nanocrystallite during thermal treatment was calculated.

Keywords: *Fabrication; Nanostructure; La_2O_3-Co_3O_4-ZrO_2; Composite; Co-precipitation.*

INTRODUCTION

Mixed metal oxides comprise the vast majority of catalysts used in modern chemical industry. Among the mixed metal oxides, Cobalt oxide (Co_3O_4) powder has a wide range of applications in various fields of industry including anode materials for rechargeable Li-ion battery, catalyst, gas sensor and magnetic materials [1–4].

The properties of Co_3O_4 in above applications are highly related to the particle size. It has been indicated that nanocrystalline Co_3O_4 is especially good for the property promotion [5]. Much effort has been made to prepare Co_3O_4 nanoparticles, including pulsed laser deposition [6], sol–gel route [7], reduction–oxidation route [8], gel hydrothermal oxidation [5], homogeneous precipitation [9], staged oxidation process [10] and cobalt salt decomposition [11,12], but through all of the above methods, nanocrystalline Co_3O_4 is more difficult and inconvenient to obtain.

In general, the potential commercial cobalt catalysts are typically composed of four components: Co metal, a small amount of a second metal, oxide promoters (alkali, rare earth, and/or transition metal oxide such as ZrO_2) and supports (Silica, Alumina or Titania) [13,14]. Modification of Zirconia by a second metal, therefore, could improve its properties as a catalyst support. Previous studies have shown that the catalytic activities of Co catalysts in CO hydrogenation were improved by the use of ZrO_2 mixed oxides such as Al_2O_3–ZrO_2 [15] and SiO_2–ZrO_2 [16]. Lanthanum, one of interesting rare earth promoters for cobalt catalyst, was reported to be beneficial for CO hydrogenation to produce long chain hydrocarbons and it showed a significant enhancement of catalytic activity owing to increase of active site dispersion [17,18]. Solid-state reaction of La and Co oxides at high temperature results in the formation of large particle size and limited degree of chemical homogeneity. Fine and homogeneous particles with high specific surface area are formed during a chemical solution process, such as citrate method, using different starting precursors, usually nitrate and an organic additive such as citric acid [19].

In this study, La_2O_3-Co_3O_4-ZrO_2 nanocomposite was prepared by Co-precipitation method. The morphologies and the crystalline structures of the La_2O_3-Co_3O_4-ZrO_2 are characterized using FE-SEM, AFM, TEM, XRD, and BET. We have suggested the optimum experimental conditions for the various composite particle syntheses.

EXPERIMENTAL

The composition of the starting solution and the experimental conditions used for ternary powders are listed in Table 1. The La_2O_3-Co_3O_4-ZrO_2 was prepared separately by mixing precursors: ($Co(No_3)_2.6h_2O$ (Merck ≥ 99%) ,Water, HNO_3)), ($ZrOCl_2$ (Merck ≥ 99%), water, acetic acid (Fluka, 60%), ethanol (Merck ≥ 99%)) , (($La(NO_3)_3$ (Fulka ≥ 99%), water, HNO_3) at room temperature and then these solutions were combined with together and after 72 h, gelation was formed. This gel also was dried for 12 h at 80°C and then was washed thoroughly with distilled water to eliminate the chloride ions. This powder calcined at 600 and 800 °C.

Table 1. Composition of starting solutions and experimental conditions for ternary powders preparation

Co-precipitation method	Precursor and Molar ratio(MR)	Stirring Time(h)	pH
	$Co(No_3)_2.6h_2O$ / $ZrOCl_2$ / $La(NO_3)_3$ =1	72	8

Characterization of the La_2O_3-$Co3O_4$-ZrO_2

XRD patterns measured on a (GBC-MMA 007 (2000)) X-ray diffractometer. The diffractograms recorded with (Kα(Cu), 1.54056Å, 0.02° step size in which the speed 10°/min) radiation over a 2θ range of 10°–70°. The N_2 adsorption–desorption isotherms are obtained by on a Sorptometer Kelvin 1042 at 77 °K, from which the surface area (S_{BET}), the pore volume (V_P) and the pore diameter (d_P) are calculated by BET and BJH methods, respectively.

RESULTS AND DISCUSSION

Crystallographic phases of the composite were investigated by XRD method. Figure 1 and assignments of the XRD peaks are summarized in Table 2, respectively. Due to different hydrothermal treatment crystalline phases are formed. Figure 1 shows the XRD patterns of powder obtained from gels after drying and calcination at 600 °C and 800 °C with 10 $\frac{\dot{c}}{min}$ gradient and stayed in 2 hours, after then, they cooled in similar temperature gradiant. Figure 1 shows the amorphous structure for as-prepared sample due to the short range ordering of the network [20]. Samples obtained from 600 °C and 800 °C have a high degree of the crystallinity. The grain size values were calculated from Scherrer equation:

$$d = \frac{0.9\,\lambda}{2B\cos\theta}, \qquad (1)$$

Where λ = 0.154 nm, and θ is the reflection angle.

As shown in Figures 1, there is only Co_3O_4 phase (peak at 2θ= 37.1°). The size of grains

increases with increasing the calcination temperature corresponds to Table 2.

Lattice strains of nanocrystallites are determined from the dependence of FWHM of diffraction lines observed in 2θ range of 10-80° on sinθ, according to the Williamson-Hall's equation [21]:

$$\beta cos\theta = \frac{k\lambda}{L} + 4sin\theta, \qquad (2)$$

Where β was FWHM observed, shape factor k was assumed to be 0.9 similar to Scherrer equation's. λ (wavelength of K_α (Cu). The plots of βcosθ against 4sinθ for different samples were approximated to be linear. Lattice strain was determined from the slop of this linear relation. Because of lowly-crystallized powder samples, the linearity between βcosθ and 4sinθ is not very evident [22]. The plots of βcosθ against 4sinθ for different diffraction lines are illustrated in Figure 2. For low calcined temperatures, the experimental points for the diffraction lines measured scattered, because the peaks are weak and broad so that their FWHMs were difficult to be measured. As can be seen in Figure 2, the lattice strain increases from 0.2597 (of 600°C) to 0.4179 (of 800°C) calcinations temperature.

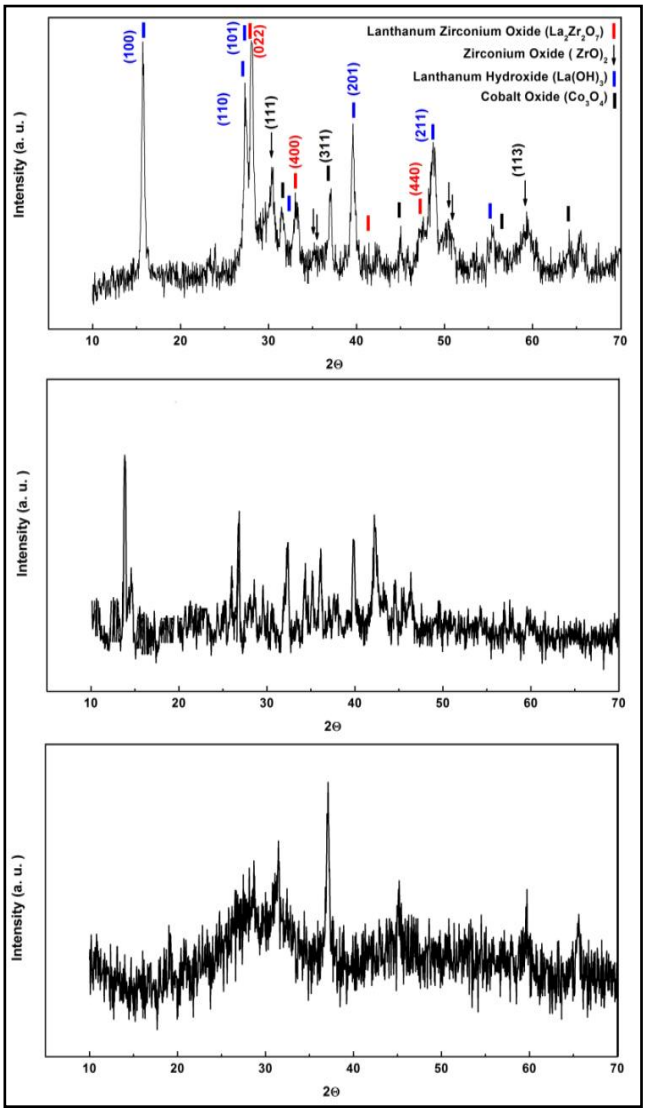

Fig. 1. XRD patterns of La_2O_3-$Co3O_4$-ZrO_2 (a) without calcination temperature (as-prepared), (b) calcined at 600 °C and (c) calcined at 800 °C.

Table 2. The 2θ angle, d-space, Miller indexes, grain size and lattice strain of La_2O_3-$Co3O_4$-ZrO_2.

Crystalline Phase	As-prepared			Calcined at 600 °C			Calcined at 800 °C		
	2Θ	d-space(Å)	size(nm)	2Θ	d-space(Å)	size(nm)	2Θ	d-space(Å)	size(nm)
$La_2Zr_2O_7$ Cubic a=10.823 Å		----------		28.08	3.15	4	28.15	3.17	4
ZrO_2 Cubic a=5.1030 Å		----------		30.61	2.91	3	30.471	2.93	4
$La(OH)_3$ Hexagonal a=6.5286 Å c=3.859 Å		----------		16.00	5.50	6	15.81	5.59	10
Co_3O_4 Cubic a=8.0840 Å	37.10	2.41	3	36.95	2.41	5	37.06	2.42	8

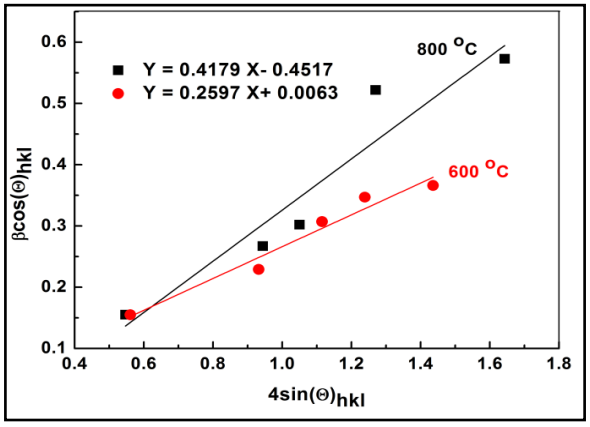

Fig. 2. The relation between βcosθ and 4sinθ (Williamson-Hall plots) with different calcination temperatures.

SEM images of La_2O_3-Co_3O_4-ZrO_2 nanopowders are shown as Figure 3(a-c). In Figure 3(a), as-prepared powder sample has irregular surface. As shown in Figure 3, SEM images of powders with different calcination temperatures are presented. Nanoparticles have more congestion and density with increasing the calcination temperature also, with increasing the calcination temperature, nanoparticles become tetragonal-shape. It is obvious that larger particle size is achieved by increasing the calcinations process and this is in good consistence with the Scherrer's equation in the XRD evaluation.

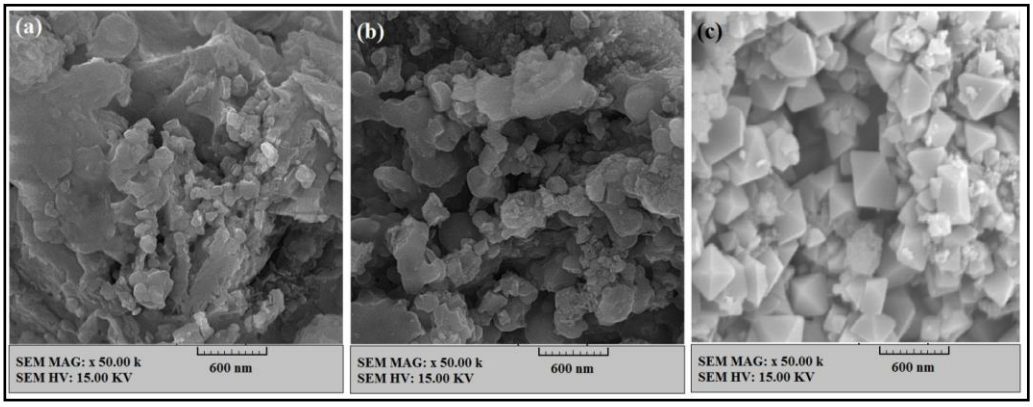

Fig. 3. SEM images of powder samples for MR=0.5 (a) as-prepared, (b) 300 °C, (c) 600 °C, (d) 800 °C.

Additional characteristic parameters of the sample with 800 °C calcination temperature (such as BET surface area, mean pore diameters) are calculated by BET and BJH methods. According to the BET method data particles have a specific surface area of 12.039 m^2/g and the mean pore diameter of 24.262 nm and total pore volume 0.07302 cm^2/g . We can notice from BJH method (Figure 4(a-c)) that the pore size distribution (peak) is 5.29 nm.

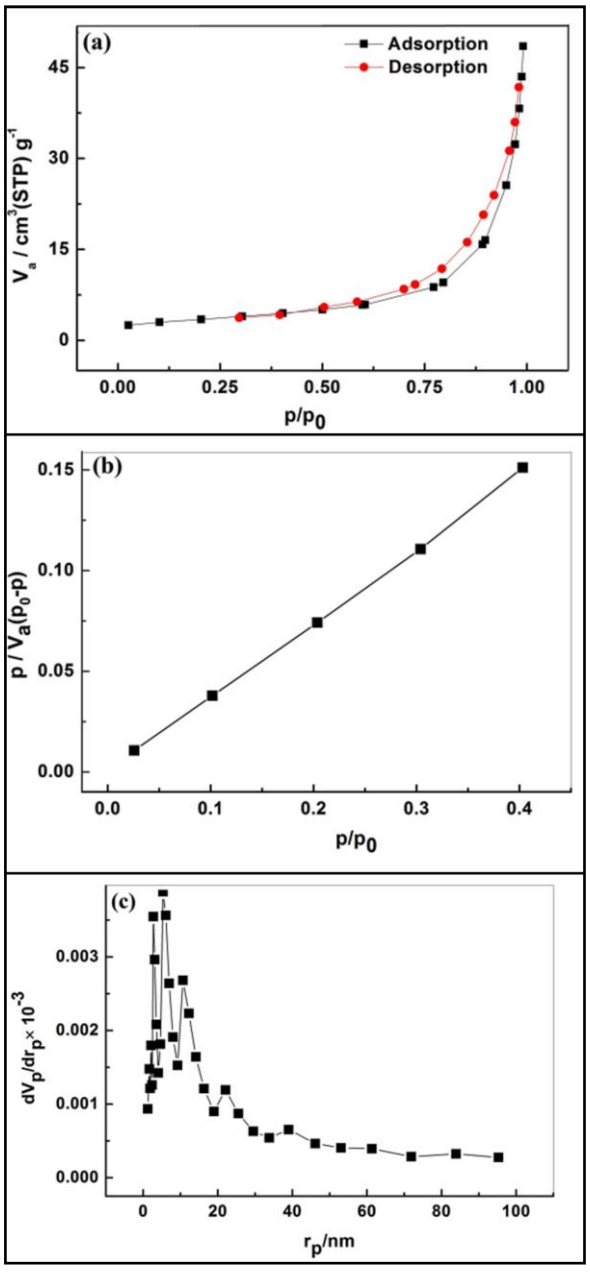

Fig.4. (a) Isotherm adsorption-desorption plot, (b) BET plot, (c) BJH plot.

CONCLUSIONS

Experimental results indicate that the homogeneous synthesis of La_2O_3-Co_3O_4-ZrO_2 composite via co-precipitation route is a promising technique for preparing material with uniform nanoparticles. In this study, nanocrystalline La_2O_3-Co_3O_4-ZrO_2 particles have been successfully synthesized by chemical method and heat treatment process. The effect of La_2O_3-Co_3O_4-ZrO_2 composite on the structural properties of powders by co-precipitation technique has been examined. The XRD spectra show $La_2Zr_2O_7$, ZrO_2, $La(OH)_3$ and Co_3O_4 phases and grains size. The size of grains increase with increasing the calcination temperature corresponds to Table 2. Scanning electron microscopy measurements show nanostructure and morphology of powders. With increasing the calcination temperature, nanoparticles become tetragonal-shape and larger particle size is achieved by increasing the calcination temperature. It has been shown that with increasing the calcination temperature lattice strain increases from 0.2597 (of 600 °C) to 0.4179 (of 800 °C) calcination temperatures.

REFERENCES

[1] Koinuma M., T. Hirae, Matsumoto Y., (1998), Electrochemical preparation of cobalt oxide using an autoclave electrolytic. *Cell. J. Mater. Res*. 13: 837-839.

[2] Jansson J., Palmqvist A. E. C., Fridell E., (2002), On the Catalytic Activity of Co_3O_4 in Low-Temperature CO Oxidation. *J. Catal*. 211: 387-397.

[3] Choi S. D., Min B. K., (2001), Co_3O_4-based isobutane sensor operating at low temperatures. *Sens. Actuators. B*. 77: 330-6.

[4] Makhlouf S. A., Magn J., (2002), Magnetic Properties of Co_3O_4 Nanoparticles, *Magn. Mater*. 246: 184-190.

[5] Jiang Y., Wu Y., Xie B., Qian Y., (2002), Moderate temperature synthesis of nanocrystalline Co_3O_4 via gel hydrothermal

oxidation. *Mater. Chem. Phys*. 74: 234-237.

[6] Koshizaki N., Narazaki A., Sasaki T., (2001), Size distribution and growth mechanism of Co_3O_4 nanoparticles fabricated by pulsed laser deposition. *Scr. Mater*. 44: 1925-1928.

[7] Svegl F., Orel B., Grabec I., Kaucıc V., (2000), Characterization of spinel Co_3O_4 and Li-doped Co_3O_4 thin film electrocatalysts prepared by the sol‐gel route. *Electrochim. Acta* 45: 4359-4371.

[8] Ni Y., Ge X., Zhang Z., Liu H., (2001), A simple reduction-oxidation route to prepare Co_3O_4 nanocrystals. *Mater. Res. Bull*. 36: 2383-3287.

[9] Zhu X., Liao L., Chui Y., (2001), One-dimensional arrays of Co_3O_4 nanoparticles: synthesis, characterization, and optical and electrochemical properties. *Inorg. Chem. Ind*. 34: 1-7.

[10] Zeng H.C., Lim Y. Y., (2000), Effect of annealing on fluorescence of Ce^{3+}-doped silica prepared by sol-gel process. *J. Mater. Res.* 15: 1250-56.

[11] Furlanetto G., Formaro L., (1995), Precipitation of Spherical Co_3O_4 Particles. *J. Collo. Interf. Sci*. 170: 169-175.

[12] Ardizzone S., Spinolo G., Trasatti S., (1995), The point of zero charge of Co_3O_4 prepared by thermal decomposition of basic cobalt carbonate. *Electrochim. Acta* 40: 2683-7.

[13] Haddad G. J, Chen B., Goodwin J. G. (1996), Characterization of La_3O_4-promoted Co/SiO_2 catalysts. *J. Catal*. 160: 43–51.

[14] Iglesia E., (1997), Design, synthesis, and use of cobalt-based Fischer–Tropsch synthesis catalysts. *Appl. Catal. A*. 61: 59–78.

[15] Soisuwan S., Panpranot J., Trimm D. L., Praserthdam P., (2006), A study of Alumina-Zriconia mixed Oxides prepared by the modified Pechini as Cobalt catalyst supports in CO hydrogenation. *Appl. Catal. A. Gen*. 303: 268–272.

[16] Jongsomjit B., Kittiruangrayub .S, Praserthdam P., (2007), Study of cobalt dispersion onto the mixed nano-SiO_2–ZrO_2 supports and its application as a catalyst phase. *Mater. Chem. Phys*. 105: 14–19.

[17] Khodakov A. Y., Chu W., Pascal F., (2007), Advance in the development of novel Fischer–Tropsch catalyst for synthesis of long chain hydrocarbon and clean fuel. *Chem. Rev*. 107: 1692–1744.

[18] Wang T., Ding Y., Lu¨ Y., Zhu H., Lin L., (2008), Influence of lanthanum on the performance of Zr–Co/ activate dcarbon catalysts on Fischer–Tropschsynthesis. *J Natur. Gas Chem*. 17: 153–158.

[19] Hwang H. J., Moon J., Awano M., Maeda K., (2000), Design of multi-layered electrochemical cell for exhaust gas purification. *J. Am. Ceram. Soc*. 83: 2852-5.

[20] Hochbaum A. I., Fan R., He R., Yang P., (2005), Controlled Growth of Si Nanowire Arrays for Device Integration. *Nano Lett.* 5: 457-460.

[21] Carp O., Huisman C. L., Reller A., (2004), Photoinduced reactivity of titanium dioxide. *Prog. Solid State Chem*. 32: 33-177.

[22] Inagaki M., Nonaka R., Tryba B., Morawski A. W., (2006), Dependence of photocatalytic activity of anatase powders on their crystallinity. *Chemosphere*. 64: 437-445.

Cite this article as: N. Aghaeenejad *et al.*: Fabrication and nano structural study on La_2O_3-Co_3O_4-ZrO_2 composite. ***Int. J.Nano Dimens.*** 6(1): 39-44, Winter 2015